Title
Activin type II receptor signaling in cardiac aging and heart failure

Journal
Science Translational Medicine, 11(482)

ISSN
1946-6234

Authors
Roh, Jason D
Hobson, Ryan
Chaudhari, Vinita
et al.

Publication Date
2019-03-06

DOI
10.1126/scitranslmed.aau8680

Peer reviewed

HHS Public Access

Author manuscript

Sci Transl Med. Author manuscript; available in PMC 2020 April 03.

Published in final edited form as:

Sci Transl Med. 2019 March 06; 11(482): . doi:10.1126/scitranslmed.aau8680.

Activin type II receptor signaling in cardiac aging and heart failure

Jason D. Roh[1], **Ryan Hobson**[1], **Vinita Chaudhari**[1], **Pablo Quintero**[2], **Ashish Yeri**[1], **Mark Benson**[2], **Chunyang Xiao**[1], **Daniel Zlotoff**[1], **Vassilios Bezzerides**[3], **Nicholas Houstis**[1], **Colin Platt**[1], **Federico Damilano**[1], **Brian R. Lindman**[4], **Sammy Elmariah**[1], **Michael Biersmith**[5], **Se-Jin Lee**[6,7], **Christine E. Seidman**[8,9,10], **Jonathan G. Seidman**[8], **Robert E. Gerszten**[2], **Estelle Lach-Trifilieff**[11], **David J. Glass**[12], **Anthony Rosenzweig**[1,*]

[1]Corrigan Minehan Heart Center, Massachusetts General Hospital, Harvard Medical School, Boston, MA 02114, USA. [2]Division of Cardiovascular Medicine, Beth Israel Deaconess Medical Center, Harvard Medical School, Boston, MA 02115, USA. [3]Department of Cardiology, Boston Children's Hospital, Harvard Medical School, Boston, MA 02115, USA. [4]Division of Cardiovascular Medicine, Vanderbilt University Medical Center, Nashville, TN 37203, USA. [5]Division of Cardiovascular Medicine, Wexner, Medical Center, Ohio State University, Columbus, OH 43210, USA. [6]The Jackson Laboratory, Farmington, CT 06032, USA. [7]Department of Genetics and Genome Sciences, University of Connecticut School of Medicine, Farmington, CT 06032, USA. [8]Department of Genetics, Harvard Medical School, Boston, MA 02115, USA. [9]Howard Hughes Medical Institute, Chevy Chase, MD 20815, USA. [10]Division of Cardiovascular Medicine, Brigham and Women's Hospital, Boston, MA 02114, USA. [11]Novartis Institutes for Biomedical Research, CH-4056 Basel, Switzerland. [12]Novartis Institutes for Biomedical, Research, Cambridge, MA 02139, USA.

Abstract

Activin type II receptor (ActRII) ligands have been implicated in muscle wasting in aging and disease. However, the role of these ligands and ActRII signaling in the heart remains unclear. Here, we investigated this catabolic pathway in human aging and heart failure (HF) using circulating follistatin-like 3 (FSTL3) as a potential indicator of systemic ActRII activity. FSTL3 is a downstream regulator of ActRII signaling, whose expression is up-regulated by the major ActRII ligands, activin A, circulating growth differentiation factor-8 (GDF8), and GDF11. In humans, we found that circulating FSTL3 increased with aging, frailty, and HF severity, correlating with an

[*]**Corresponding author.** arosenzweig@partners.org.

Author contributions: J.D.R., P.Q., and A.R. designed the research. J.D.R., P.Q., C.X., D.Z., V.B., N.H., and F. D. performed in vivo experiments. J.D.R., R.H., and V.C. performed in vitro experiments. J.D.R., R.H., P.Q., A.Y., M. Benson, N.H., C.P., V.B., and M. Biersmith analyzed data. F.D., B.R.L., S.E., S.-J.L., C. E.S., J.G.S., R.E.G., E.L.-T., and D.J.G. provided guidance on experimental designs and data analyses. J.D.R. and A.R. wrote the manuscript. All authors provided feedback on the manuscript.

Data and materials availability: All data associated with this study are present in the paper or the Supplementary Materials. RNA-seq and proteomics datasets have been deposited in SRA (PRJNA518904) and dbGaP (pht006013.v1.p10). Ad. activin A and ActRIIB-floxed mice are available under a material transfer agreement with MGH (A.R.) and University of Connecticut School of Medicine (S.-J.L.), respectively. CDD866 and RAP-031 are proprietary materials of Novartis and Acceleron, respectively, and may be shared under material transfer agreement under restricted industry standard conditions.

SUPPLEMENTARY MATERIALS

www.sciencetranslationalmedicine.org/cgi/content/full/11/482/eaau8680/DCl

increase in circulating activins. In mice, increasing circulating activin A increased cardiac ActRII signaling and FSTL3 expression, as well as impaired cardiac function. Conversely, ActRII blockade with either clinical-stage inhibitors or genetic ablation reduced cardiac ActRII signaling while restoring or preserving cardiac function in multiple models of HF induced by aging, sarcomere mutation, or pressure overload. Using unbiased RNA sequencing, we show that activin A, GDF8, and GDF11 all induce a similar pathologic profile associated with up-regulation of the proteasome pathway in mammalian cardiomyocytes. The E3 ubiquitin ligase, Smurf1, was identified as a key downstream effector of activin-mediated ActRII signaling, which increased proteasome-dependent degradation of sarcoplasmic reticulum Ca^{2+} ATPase (SERCA2a), a critical determinant of cardiomyocyte function. Together, our findings suggest that increased activin/ActRII signaling links aging and HF pathobiology and that targeted inhibition of this catabolic pathway holds promise as a therapeutic strategy for multiple forms of HF.

INTRODUCTION

Heart failure (HF) is a major cause of morbidity and mortality, with growing prevalence due to the aging of populations worldwide (1). Despite currently available therapies, prognosis remains poor for many patients with HF. Five-year mortality rates range from ~40 to 75% after a HF-associated hospitalization (1–3). Although multiple factors contribute to the increasing prevalence of HF, advanced age remains one of its strongest risk factors (1). The mechanisms by which aging contributes to the development of HF, and whether it is possible to intervene effectively in this process, however, remain largely unclear.

In this context, the role of activin type II receptor (ActRII) ligands has been a subject of intense interest and controversy. Recently, circulating growth differentiation factor-11 (GDF11), an ActRII ligand, was reported to decline with age in humans and mice (4–6). Despite its known catabolic properties, exogenous GDF11 reversed pathologic cardiac hypertrophy, sarcopenia, and exercise intolerance in old mice (4, 7), suggesting that an age-related decline in GDF11 and ActRII signaling might contribute to these pathologies. Similarly, Oshima and colleagues (8) suggested that activin A, another ActRII ligand, could be cardioprotective, although the effects on cardiac function were not examined.

Subsequent studies have questioned these findings. Using a highly specific mass spectrometry assay for GDF8 and GDF11, Schafer and colleagues (9) found that the reported age-associated changes in circulating GDF11 predominantly reflected decreases in the structurally similar GDF8, whereas GDF11 did not change with age in humans. However, other relevant ActRII ligands were not measured, and overall pathway activity was not assessed. Previous work from our group and others has also demonstrated that genetic deletion of GDF8 improves cardiac function in senescent mice (10, 11), suggesting that decreased GDF8 would be beneficial and unlikely to contribute to the association between aging and HF. GDF11's putative anti-aging effects in cardiac and skeletal muscle have also been questioned (12–14), as have the cardioprotective effects of activin A (15–18).

Thus, how ActRII activity changes in human aging and disease and the functional implications of this pathway in the heart remain unclear. Here, by focusing on the common signaling mechanisms of ActRII ligands and using circulating follistatin-like 3 (FSTL3) as a

potential indicator of pathway activation, we provide evidence, suggesting that systemic ActRII activity increases in human aging, frailty, and HF, and identify activins as one of the major ligands driving this age-related phenomenon. Gain- and loss-of-function studies in animal models of aging and HF establish ActRII activation as causally related to cardiac dysfunction and demonstrate that targeted inhibition of this pathway can restore function to the failing heart.

RESULTS

FSTL3 increases in human aging

Assessing the impact of circulating ActRII ligands in humans is complicated by their binding to endogenous inhibitors or pro-domains, which inhibit their ability to bind and activate ActRII (19, 20). Current assays have limited specificity for bioactive forms of ActRII ligands (9); thus, measuring circulating ligand concentrations alone may not necessarily provide the most accurate representation of overall pathway activity. In addition, expression patterns of the various ActRII ligands can change in opposing directions as part of this pathway's complex regulatory network, which makes inferring the overall impact of discordant changes in multiple ligands challenging. Thus, to gain deeper insight into how age-associated changes in circulating ActRII ligands affect overall pathway activity in humans, we measured them concurrently with circulating FSTL3. Although FSTL3 is an endogenous inhibitor of ActRII ligands (20–24), its expression is strongly up-regulated by all of the major ligands through ActRII-induced Smad2/3 signaling (23, 25), suggesting that circulating FSTL3 could provide an indirect indication of systemic pathway activity. FSTL3 can also be induced by other signals, such as transforming growth factor-β (TGFβ) (26), so it cannot be equated with ActRII signaling in all settings. However, correlation of FSTL3 with relevant circulating ligands (including ActRII ligands and TGFβ) can help identify the most likely drivers of FSTL3 expression.

Using this strategy, we examined a plasma proteomics analysis of 899 individuals from the Framingham Heart Study (FHS) (27) to determine whether circulating FSTL3 changes with age in humans. FSTL3 increased from age 29 to 82 in this population (Fig. 1A). To then determine which ligands might be driving this process, we examined the association of FSTL3 with circulating activins, GDF8 + GDF11 (a composite measure of both proteins because they are not individually differentiated in this assay), as well as TGFβ. Although activins and GDF8 + GDF11 displayed opposing associations with age and sex (Fig. 1A and table S1), after adjusting for these variables, activins were the only ligands positively correlated with FSTL3 (Fig. 1B). GDF8 + GDF11 negatively correlated with FSTL3, and TGFβ showed no correlation. Together, these findings suggest that systemic ActRII activity, as indicated by circulating FSTL3 measurements, increases with age and is likely driven by an age-related increase in activins, as opposed to GDF8 + GDF11 or TGFβ.

FSTL3 increases with HF severity and frailty in humans

To determine whether circulating FSTL3 increases in HF, we used a similar proteomics platform in an independent cohort of 50 adults, ages 39 to 95, with severe aortic stenosis (AS) and HF (table S2). Similar to our findings in the FHS cohort, FSTL3 increased with

age (Fig. 1C) and only positively correlated with activins (fig. S1). After adjusting for age and sex, FSTL3 and activins both correlated with worsening HF, as indicated by New York Heart Association (NYHA) functional class or N-terminal pro–B-type natriuretic peptide (NT-proBNP; Fig. 1, C and D). In contrast, GDF8 + GDF11 negatively correlated, and TGFβ had no association with these HF metrics (fig. S2). These data suggest that systemic ActRII activity, as indicated by circulating FSTL3, increases in relation to HF severity and that, as with the age-related increase seen in the FHS cohort, activins are the principal ligands driving this increase.

Frailty, a geriatric syndrome reflective of biological aging and declining physiological reserves, provides powerful prognostic information in older patients with AS (28). We measured plasma FSTL3 and activin A concentrations in an independent age- and sex-matched cohort of older patients with AS/HF, with (n = 21) or without (n = 22) frailty (table S3). Frail individuals, defined by slow walk speed and weak handgrip strength, had higher FSTL3 (Fig. 1E), suggesting that systemic ActRII activity is also likely increased in frailty in older patients with HF.

Circulating activin A and cardiac ActRII signaling increase in murine aging and HF

Although clinical correlations suggested that activin-mediated ActRII activity increases with aging and HF, inferences from cross-sectional analyses of circulating biomarkers are limited, and documentation of cardiac activation ultimately requires direct assessment of tissue. To address this, we examined aged C57BL/6 mice, an established model of cardiac aging (29, 30). Compared to young (4-month-old) mice, old (28-month-old) mice had ~3-fold higher circulating activin A concentrations, which was associated with increased cardiac FSTL3 expression and Smad3 phosphorylation, indicating increased ActRII signaling in the aged heart (Fig. 2, A to C). No significant differences were observed in cardiac activin A, GDF11, or TGFβ expression in aged animals (Fig. 2B), suggesting that the increased circulating activin A (and consequent increased cardiac ActRII signaling) seen in old mice largely originates from outside the heart. Circulating GDF8 decreased with age and was associated with decreased skeletal muscle mass (fig. S3), suggesting that the age-related decline in circulating GDF8, seen in both mice and humans (9), likely represents a secondary effect of age-related sarcopenia. These findings corroborate our observations in humans and demonstrate that cardiac ActRII signaling is increased in the aged heart.

We also examined ActRII signaling in a transverse aortic constriction (TAC) model of left ventricular (LV) pressure overload, which exhibits similar pathophysiology to the human AS populations studied, with the caveats that increased afterload is generated more distally within the aortic arch in the TAC model and progresses more rapidly than clinical AS. One week after TAC, circulating activin A increased ~2-fold and was associated with increased cardiac FSTL3 expression and ActRII activity (Fig. 2, D to F). Consistent with previous reports (8) and in contrast to the aging model, cardiac activin A expression increased after TAC (Fig. 2E), indicating both local and systemic up-regulation in this model. Thus, both aging and biomechanical cardiac stress can induce activin expression, leading to activation of cardiac ActRII signaling and a corresponding increase in cardiac FSTL3 expression.

Increased circulating activin A is sufficient to induce cardiac dysfunction

To examine the functional effects of increased cardiac activin/ActRII signaling, we injected 4-month-old mice with recombinant adenoviral vectors encoding activin A (Ad.activin A) or control green fluorescent protein (Ad.GFP). Ad.activin A increased circulating activin A to supraphysiologic concentrations (Fig. 3A) and activated cardiac ActRII signaling, as well as increased FSTL3 expression in cardiac and skeletal muscle without increasing tissue-specific expression of ActRII ligands (Fig. 3, B and C, and fig. S4). Although circulating activin A concentrations were higher than seen in most human HF (15), they were comparable to concentrations seen in some human cardiovascular diseases associated with cardiac dysfunction (31) and were sufficient to impair both systolic and diastolic cardiac function in otherwise healthy young mice (Fig. 3, D and E) without significantly affecting blood pressure ($P = 0.53$; fig. S5A). Lung weight was also increased in activin A–overexpressing mice, consistent with pulmonary congestion and HF (Fig. 3F).

GDF11 induces cardiac dysfunction in aged mice

Although our data demonstrated that increased activin A/ActRII signaling impairs cardiac function, previous reports proposed that other ActRII ligands such as GDF11 improve remodeling and function in the aged or injured heart (4, 32). To determine whether our observations were unique to activin A, we examined the functional effects of GDF11 using a protocol similar to previous reports (4) (fig. S6A). Recombinant GDF11 bioactivity was confirmed in neonatal rat ventricular myocytes (NRVMs; fig. S6, B and C), and matched 24-month-old C57BL/6 mice were treated with vehicle or GDF11 (table S4). Similar to previous reports, we found that GDF11 increased ActRII signaling in the aged heart, reduced cardiac mass and cardiomyocyte (CM) size, and up-regulated atrogene expression (Fig. 3G and fig. S6, D to G). However, similar to activin A overexpression, GDF11 impaired cardiac function, did not improve functional HF phenotypes or adverse cardiac remodeling, and induced skeletal muscle atrophy (Fig. 3, H and I, and fig. S6, H to J). Thus, activin A and GDF11 induce similar effects in the mammalian heart, and either is independently sufficient to induce cardiac dysfunction and pathologic atrophy.

Systemic ActRII inhibition improves systolic function in murine age-related HF models

We next examined whether ActRII inhibition could improve cardiac functional impairments seen in old C57BL/6 mice (29, 30) using a murinized version of bimagrumab (CDD866), a monoclonal antibody (Ab) that blocks ActRIIA and ActRIIB and is currently under clinical investigation for sarcopenia (Fig. 4A) (33, 34). Similar to its effects in young mice (34), CDD866 increased skeletal muscle mass but did not significantly alter cardiac mass or blood pressure in old mice (figs. S5 and S7). CDD866 effectively blocked cardiac ActRII signaling (Fig. 4B) and reduced pulmonary congestion (Fig. 4C). CDD866 also improved subclinical LV systolic dysfunction, including measures of systolic strain and contractile reserves (Fig. 4, D and E), although diastolic function and chronotropic reserves were not altered.

Because CDD866 mostly affected systolic function, which is only modestly altered in aged C57BL/6 mice, we explored its effects in an age-related model of dilated cardiomyopathy based on a known myosin heavy chain missense mutation (MHCF764L) found in humans (35). Knock-in mice heterozygous for this mutation develop progressive LV dilatation and

systolic dysfunction with age. Treating these mice (21 to 23 months old) with CDD866 decreased cardiac ActRII signaling (Fig. 4F) and increased FS by ~45% within 4 weeks (Fig. 4G).

The marked effects of CDD866 in aged MHCF764L mice prompted us to repeat these studies with an ActRIIB-Fc fusion protein, RAP-031, to ensure that the effect was not reagent specific. RAP-031 is a soluble ligand trap that blocks pathway activation by binding circulating ActRII ligands (Fig. 4A) (36). Four weeks of RAP-031 treatment induced results similar to CDD866, increasing FS by ~34% (Fig. 4H).

Systemic ActRII inhibition preserves and restores systolic function in LV pressure overload

Given the cardiac functional effects seen with ActRII inhibitors in MHCF764L mice, we tested them in a more severe model of systolic HF induced by TAC. In an initial prevention study (Fig. 5A), CDD866 had no effect on baseline cardiac function but substantially mitigated the decline in systolic function induced by TAC (Fig. 5, B and C). Hearts explanted 11 weeks after TAC had ~3-fold increased FSTL3 expression, confirming chronic ActRII activation in this HF model, which was completely abrogated by CDD866 (Fig. 5D). Furthermore, mice treated with CDD866 demonstrated attenuated pathologic gene expression profiles and improved survival (Fig. 5, E to H, and fig. S8, A and B).

In a more clinically relevant treatment protocol (treatment initiated after FS declined to <45%; Fig. 5I), CDD866 improved systolic function within 2 weeks, which was sustained over the 8-week time course (Fig. 5J). CDD866 decreased cardiac FSTL3 expression and pulmonary congestion (Fig. 5, K to N, and fig. S8, C and D), suggesting that systemic ActRII inhibition can rescue cardiac function and pulmonary edema in established HF.

To confirm that the cardiac effects induced by CDD866 in TAC were not strain or reagent specific, we repeated these studies in FVB mice with RAP-031. Although the effect size was smaller, reflecting less severe cardiac dysfunction in FVB mice after TAC, RAP-031 similarly improved systolic function in TAC-induced HF (fig. S9).

CM-specific ActRIIB deletion attenuates cardiac dysfunction in TAC

To determine whether the beneficial cardiac effects of these pharmacological inhibitors are directly mediated at the CM level, we generated CM-specific ActRIIB knockout (CS-ActRIIB-KO) mice based on previous evidence, suggesting that ActRIIB has stronger ligand affinity than ActRIIA (37). CS-ActRIIB-KO mice displayed normal cardiac structure and function at baseline (fig. S10) but were substantially protected from systolic dysfunction after TAC (Fig. 5, O and P). Eight weeks after TAC, cardiac function in CS-ActRIIB-KO mice began to decline but remained better than controls, without significantly reduced cardiac FSTL3 or pathologic gene expression profiles (Fig. 5, P to S). These data suggest that the inhibition of CM ActRIIB contributes to the functional benefits observed with either systemic treatment. However, the less sustained protection and non-significant impact on late gene expression suggest that cardiac ActRIIA also likely contributes, although a role for non-CM ActRII signaling or cell nonautonomous effects cannot be excluded. In a practical

sense, inhibition of both receptors is likely optimal to maximizing therapeutic potential in the heart, as has been reported in skeletal muscle (34).

ActRII ligands induce a similar pathologic profile in mammalian CMs

Given evidence for direct effects on CMs, we used RNA sequencing (RNA-seq) to identify mechanisms by which ActRII ligands (GDF8, GDF11, and activin A) might mediate their effects in primary CMs. All three ligands increased FSTL3 expression (>3-fold) and induced similar transcriptional profiles (Fig. 6A and table S5). Consistent with our in vivo findings, pathway analysis revealed a conserved biological signature induced by all three ligands that was consistent with a HF phenotype, including up-regulation of multiple cardiomyopathy pathways and down-regulation of oxidative phosphorylation and fatty acid metabolism, cardiac muscle contraction, and Ca^{2+} signaling pathways (Fig. 6, B and C, and tables S6 and S7).

ActRII signaling regulates proteasome-mediated degradation of SERCA2a

The consistent evidence suggesting detrimental effects of chronically activated ActRII signaling on CM function seemed at odds with previous reports in which GDF11 increased mRNA expression of sarcoplasmic reticulum Ca^{2+} ATPase (SERCA2a), a powerful regulator of CM excitation-contraction coupling (4). To investigate this further, we measured cardiac SERCA2a mRNA expression in our GDF11-treated mice and found that it was higher than controls (Fig. 7A). However, SERCA2a protein was reduced by GDF11 treatment (Fig. 7A). Hearts from Ad.activin A–treated mice also had lower SERCA2a protein (Fig. 7B), which corresponded with marked impairments in CM function and Ca^{2+} cycling (Fig. 7C and movies S1 and S2). Conversely, ActRII inhibition with CDD866 increased SERCA2a protein in both aging and TAC models without significantly affecting mRNA expression (Fig. 7, D and E).

Activin A induced similar results in primary CMs. Although activin A decreased SERCA2a mRNA expression in vitro, this effect plateaued at 25 ng/ml (fig. S11A), whereas SERCA2a protein declined further at higher concentrations (Fig. 8A). CDD866 similarly blocked activin A–induced reduction in SERCA2a protein without affecting mRNA expression (Fig. 8B and fig. S11B), confirming that ActRII ligands regulate SERCA2a expression at a posttranscriptional level and directly through CM ActRII.

Given that the proteasome was among the most highly up-regulated pathways by all three ActRII ligands (Fig. 6C and table S6), we hypothesized that our SERCA2a findings might be explained by ActRII-mediated proteasome regulation. Proteasome inhibition with MG132 almost completely abrogated the effects of activin A on SERCA2a protein expression (Fig. 8C). Although activin A did not directly increase proteasome activity in CMs (Fig. 8D), it increased ubiquitination of SERCA2a by ~3.4-fold (Fig. 8E), implicating a likely role for ActRII-targeted ubiquitin E3 ligase activity. Review of the RNA-seq dataset identified a small number of E3 ligases up-regulated in CMs by multiple ActRII ligands (table S5). One of these, Smad-specific E3 ubiquitin protein ligase 1 (Smurf1), was particularly intriguing given a previous link to activin and Smad signaling (38), along with availability of a selective small-molecule inhibitor. Smurf1 inhibition recapitulated the benefits of MG132 in

blocking activin A–induced reductions in SERCA2a protein, suggesting a key role of the activin/ActRII/Smurf1 axis in regulating CM SERCA2a (Fig. 8F). Together, these data suggest that activation of ActRII signaling induces a pathologic phenotype in mammalian CMs as evidenced by an induction of a HF transcriptional profile, impaired function, and potent increases in SERCA2a degradation (fig. S12).

DISCUSSION

The role of the catabolic ActRII pathway in human aging and heart disease has been highly controversial due to conflicting reports on its circulating ligands and limited information regarding its in vivo functional consequences in the heart. Using multiple human cohorts, we confirmed previous reports (5, 6) that circulating combined levels of GDF8 and GDF11 decline in human aging and HF but also found that circulating activins, another major ActRII ligand, significantly increase in these same contexts. To better assess the potential impact of this discordant profile of circulating ActRII ligands on overall pathway activity, we took advantage of a common counter-regulatory mechanism induced by all the major ActRII ligands assayed; specifically, their ability to increase FSTL3 expression. Using circulating FSTL3 as a potential indicator of increased ActRII-induced Smad2/3 signaling, our data suggest that despite the associated decline in circulating GDF8 + GDF11, overall systemic ActRII activity appears to increase in human aging, frailty, and HF and is likely driven by an age-related increase in activins.

Of note, recent studies have identified similar age-related changes in circulating FSTL3 and ActRII ligands but have proposed starkly different interpretations, suggesting that the decline in GDF11 (or GDF8) and increase in FSTL3 could indicate a decrease in cardiac ActRII activity, which contributes to the pathogenesis of heart disease in the elderly (5, 6). Because FSTL3 expression is induced by ActRII activation but also functions as a negative regulator of pathway activity, it is impossible to determine definitively the impact of its circulating expression on net pathway activation in the absence of tissue samples. However, our data from a broad range of in vitro and in vivo models in which ActRII signaling can be directly assessed strongly support the value of FSTL3 as an indicator of ActRII activation. In CMs, Smad3 phosphorylation and FSTL3 expression were induced by all of the major ligands assayed. Similarly, increasing circulating activin A in mice increased cardiac FSTL3 expression, which was concordant with changes in Smad3 phosphorylation. Moreover, we found cardiac ActRII signaling to be increased in established animal models of aging and HF, making it highly improbable that a decrease in circulating GDF8 or GDF11 could account for the increase in cardiac FSTL3 expression or Smad3 phosphorylation seen in these contexts. Thus, the most plausible synthesis of all the available data is that ActRII signaling increases in aging and HF, which is reflected in higher FSTL3 expression, and that declining circulating GDF8 concentrations more likely represent a secondary effect of progressive muscle loss in these contexts.

With data implicating activins as one of the possible mediators of increased FSTL3 in human aging and HF, we increased circulating activin A concentrations in mice to determine its in vivo functional consequences. Increasing circulating activin A alone was sufficient to increase cardiac ActRII signaling, FSTL3 expression, and impair cardiac function in

otherwise healthy young mice. GDF11 induced similar functional changes in old mice, suggesting that circulating ActRII ligands have common effects in the heart. RNA-seq analyses in isolated CMs corroborated these findings, identifying a common biological signature induced by activin A, GDF11, and GDF8 that was consistent with a HF phenotype. Thus, although it is possible that ActRII ligands also have some distinct functions (39), our data suggest that they share adverse cardiac functional effects in vivo and induce a pathological gene expression profile in mammalian CMs in vitro.

To assess the therapeutic potential of targeting ActRII signaling in HF, we independently tested two pharmacological reagents (CDD866 and RAP-031) capable of inhibiting a broad spectrum of ActRII ligands. Both reagents have been evaluated in early clinical trials for sarcopenia (33, 36), underscoring the translational relevance of these approaches. Both reagents consistently improved cardiac function in multiple HF models and restored function in failing hearts induced by pressure overload or a clinically relevant sarcomere mutation. These functional effects were recapitulated with two different inhibitors in three different HF models in two strains of mice and with CM-specific ActRIIB deletion in TAC.

Given the breadth of cardiac conditions sensitive to ActRII modulation, we believe chronic overactivation of this pathway likely impairs processes fundamental to CM function. Although this initially seemed discordant with previous reports that GDF11 increased SERCA2a mRNA (4), we found that ActRII signaling decreased SERCA2a protein, suggesting that the increased SERCA2a mRNA seen with GDF11 treatment is likely compensatory. Our data show that the primary mechanism by which ActRII signaling regulates CM SERCA2a is through enhanced proteasome-mediated degradation (fig. S12), although a contribution from decreased protein translation cannot be excluded. Overall, our findings are more consistent with known ActRII biology in skeletal muscle (40), as well as recent data implicating Smurf1 in cardiovascular disease (41). Although our RNA-seq analyses suggest that ActRII signaling modulates multiple biological processes important for CM function, on the basis of previous experimental data (42), we believe that the changes in SERCA2a associated with ActRII modulation are a major contributor to the functional changes observed in our in vivo models. Together, these data not only identify a key mechanism by which ActRII signaling regulates cardiac function but also support an emerging theme in HF therapeutic development, which suggests that enhancing protein stability of critical proteins such as SERCA2a may be as effective as targeting their production (43).

Ultimately, our findings resolve a major controversial question of whether stimulation or inhibition of ActRII signaling will be beneficial in HF. Previous work had suggested that acute increases in activin A could be cardioprotective (8) and that GDF11 might be beneficial in age-related HF (4). However, neither study extensively assessed the impact on cardiac function. Given our finding that both activin A and GDF11 induce cardiac atrophy and decrease SERCA2a protein, which is responsible for much of the heart's energy consumption, it seems likely that these effects will reduce myocardial energy requirements. However, whatever short-term benefits this might confer will inevitably come at the expense of cardiac function. Our data demonstrate that chronic ActRII activation, as seen in aging and HF, is maladaptive and contributes to a decline in cardiac function. Thus, we propose

that the ActRII pathway likely represents another example of a partially compensatory pathway that becomes maladaptive in HF, as is well documented in neurohormonal systems. Of note, virtually all HF treatments that improve clinical outcomes inhibit such maladaptive pathways (44). Our study provides fundamental in vivo evidence that ActRII pathways may represent a new class of therapeutic targets that reflect similar HF pathophysiology.

In addition, similar to the recognition that there are distinct forms of cardiac growth, termed physiologic and pathologic hypertrophy (45), with very different functional outcomes, these data now suggest there is likely a parallel dichotomy in the reversal of such processes. A reduction in cardiac mass could result from restoration of the normal baseline physiological state or from atrophy, with distinct consequences for cardiac function and clinical outcomes. Given the catabolic effects of ActRII signaling in skeletal muscle (40), it makes sense that it would drive similar proteolytic processes in the heart that not only lead to reductions in critical functional proteins (SERCA2a) but also an overall pathologic state.

Although this study provides proof-of-principle evidence that ActRII inhibition can improve cardiac function in HF, the optimal approach for targeting this pathway in HF still needs to be defined. In addition, we acknowledge certain limitations of our study. Our human analyses primarily focused on three of the major ActRII ligands, including TGFβ, and were limited by the coverage of the proteomics platform used, which does not include all ActRII ligands and did not distinguish between GDF8 and GDF11. Recent studies have addressed the GDF8/11 aptamer issue (9), but it is possible that other ActRII ligands, in addition to activins, may be driving the increase in circulating FSTL3 seen in human aging and HF. Because of the lack of cardiac or skeletal muscle tissue specimens in our clinical cohorts, we also cannot definitively establish that the increased plasma FSTL3 observed in human aging, frailty, and HF is a direct result of increased FSTL3 expression or net ActRII pathway activation from these target tissues. However, the concordance between cardiac FSTL3 expression and canonical Smad3 signaling seen in a range of in vitro and in vivo models performed in our study, along with the well-established regulation of FSTL3 expression (25, 26), provide strong evidence to support the concept that FSTL3 levels in many contexts may reflect ActRII activity. Last, although we tested multiple HF models, we recognize that ActRII signaling may not be relevant to other subtypes (such as ischemic cardiomyopathies) that were not specifically examined and have shown varying responses to ActRII ligands and other TGFβ family members (8, 32, 46).

In summary, this study documents an age-related increase in cardiac ActRII activity that plays a causal role in HF pathobiology. We identified a key mechanism by which ActRII signaling regulates CM function through proteasome-mediated degradation of SERCA2a and present evidence with clinical-stage inhibitors that targeted ActRII blockade can restore cardiac function in HF.

MATERIALS AND METHODS

Study design

We started by examining a proteomics dataset from the FHS (27) to assess how the major ActRII ligands and FSTL3, a potential indicator of ActRII activity, change with age in

humans. These analyses were then extended to two independent cohorts of patients with AS to assess for correlations with HF and frailty. To investigate causality of cardiac ActRII activity in regulating cardiac function in aging and HF, we performed a series of gain- and loss-of-function studies in murine models. Study design, number of mice, and sample sizes used for functional and tissue analyses in the various animal studies are provided in figure legends. Human studies were approved by the Massachusetts General Hospital (MGH), Beth Israel Deaconess Medical Center (BIDMC), and Washington University Institutional Review Boards, and informed consent was obtained from all participants. Animal studies were approved by MGH and BIDMC Institutional Animal Care and Use Committees. Individual subject-level data are reported in data file S1.

Protein measurements in human blood samples

Plasma proteomic data using the SOMAscan platform were available on 899 individuals (ages 29 to 82) from the FHS Offspring Cohort (27). Quantification of FSTL3, INHBA (recognizes activin A/AB/AC), GDF8 + GDF11 (recognizes GDF8 and GDF11), and TGFβ (recognizes TGFβ−1/2/3 isoforms) was reported using aptamer IDs 3438–10, 2748–3, 2765–4, and 2333–72, respectively. Similar plasma proteomic profiling was performed on 50 adults with severe AS and HF (table S2). FSTL3 and activin A were also measured by ELISAs (R&D Systems) in 43 older patients with AS phenotyped for frailty (table S3). Frailty was defined as walk speed of <0.8 m/s and handgrip strength of <16 kg (female) or <26 kg (male).

Murine models

C57BL/6J, FVB/NJ, and αMHC*cre* mice were purchased from the Jackson Laboratory. Aged C57BL/6 mice were provided by the National Institute on Aging or purchased from the Jackson Laboratory. MHCF764L mice were provided by the Seidman Lab (35). ActRIIB-floxed mice were provided by S.-J.L. (47) and backcrossed to C57BL/6 before crossing with αMHC*cre*.

Murine interventions

Sham and TAC surgeries were performed using previously published methods (42, 45). Briefly, thoracotomy was performed in anesthetized animals, and TAC was performed by ligating the transverse aortic arch with a 27-gauge needle between the innominate and left common carotid arteries. The following reagents were used in mice: (i) Adenoviral constructs for activin A or GFP were created using a cytomegalovirus promoter and administered retro-orbitally at ~100 μl (10^{10} colony-forming units/ml); (ii) recombinant GDF11 (0.1 mg/kg; 120–11, PeproTech) or vehicle was administered daily via intraperitoneal injection; (iii) CDD866 or isotype Ab (20 mg/kg; Novartis) was delivered weekly via subcutaneous injection; and (iv) RAP-031 or vehicle (10 mg/kg; Acceleron) was administered subcutaneously twice weekly.

Murine echocardiography

Echocardiography was performed on unanesthetized mice using either a Vivid7 or an E90 cardiac ultrasound system (GE Healthcare) equipped with an i13L or L8–18i-D transducer.

Speckle-tracking strain analysis was performed on two-dimensional short-axis images using EchoPACS software (version 201, GE Healthcare). Peak systolic strain was averaged from the peak value of segmental strain curves at aortic valve closure. Early diastolic strain rate was averaged from the peak value of the segmental strain rates at 33% into diastole.

Exercise testing

Exercise capacity and cardiac reserves were measured using a stress echocardiography protocol in which mice were run to exhaustion on a treadmill (Columbus Instruments) and then imaged via echocardiography within 30 s of peak exercise. Protocol consisted of a warm-up (duration, 5 min; incline, 10°; speed, 5 m/min) and run-to-exhaustion phase (incline, 10°; speed ramp, 2 m/min/min). Exercise capacity was quantified as total work completed. Peak heart rate was averaged over nine cardiac cycles to evaluate chronotropic reserves. Percentage change in FS at peak exercise compared to rest was used to determine contractile reserves.

NRVM studies

Neonatal rats were purchased from Charles River Laboratories, and NRVMs were isolated using previously published techniques (45). NRVMs were serum starved for 6 hours before 18-hour treatment, unless otherwise specified. The following reagents were used: activin A (0 to 100 ng/ml: 338 AC, R&D Systems), GDF11 (100 ng/ml: 120–11, PeproTech), GDF8 (100 ng/ml: 788G8, R&D Systems), CDD866 (0 to 100 μg/ml; Novartis), MG132 (10 μM; Sigma-Aldrich), and A01 (10 μM; Sigma-Aldrich). Proteasome activity was measured using the 20S Proteasome Activity Assay (MilliporeSigma).

CM contractility and Ca^{2+} flow analyses

CM contractility and Ca^{2+} analyses were performed using previously published methods (48). CMs were incubated with 0.2 μM Fluo-4 AM dye (Thermo Fisher Scientific) and paced with 10 V at 1.0 Hz (C-Pace EM Stimulator, IonOptix). Lives image were acquired using a TCS SP8 confocal microscope (Leica), and image analysis was performed using ImageJ [National Institutes of Health (NIH)].

Histology and immunohistochemistry

Mid-ventricular sections were stained with wheat germ agglutinin, periodic acid–Schiff, Masson's trichrome, rabbit–anti-mouse CD31 (1:50; 77699, Cell Signaling Technology), rabbit–anti-human CD45 (1:100; 10558, Abcam), or goat–anti-human ActRIIB (1:50; PA5–47005, Thermo Fisher Scientific). CM cross-sectional area (~250 cells per heart) and capillary density were measured from three to six randomly selected sections per heart using ImageJ (NIH). Fibrosis and leukocyte content were quantified from full mid-ventricular section (KEYENCE BZ-X Analyzer). Image analysis was blinded.

Quantitative real-time polymerase chain reaction

RNA was isolated with TRIzol. Polymerase chain reaction (PCR) reactions were carried out using SYBR green and standard amplification protocols. Gene expression was normalized to

RPS18 or GAPDH and calculated using the $\Delta\Delta C_t$ method. Primer sequences are included in table S8.

Immunoblotting

Protein was isolated using radioimmunoprecipitation assay (RIPA) buffer and standard Western blotting protocols. Image quantification was performed with the ChemiDoc system (Bio-Rad). All protein expression was normalized to GAPDH or vinculin. The following primary Abs were used: mouse–anti-canine SERCA2 (1:1000; MA3–919, Thermo Fisher Scientific), rabbit–anti-human SERCA2a (1:20,000; A010, Badrilla), rabbit–anti-human SERCA2a (1:3000; Hajjar Laboratory), rabbit–anti-human Smad3 (1:1000; 9513, Cell Signaling Technology), rabbit–anti-human phospho-Smad3 ($Ser^{423/425}$) (1:1000; 9520, Cell Signaling Technology), mouse–anti-human vinculin (1:5000; V9264, Sigma-Aldrich), and rabbit–anti-human GAPDH (1:5000; 2118, Cell Signaling Technology).

Ubiquitin immunoprecipitation

RIPA buffer supplemented with protease/phosphatase inhibitor (Thermo Fisher Scientific), 1 mM phenylmethylsulfonyl fluoride (Sigma-Aldrich), and 20 mM *N*-ethylmaleimide (Thermo Fisher Scientific) was used to extract protein from NRVMs incubated with recombinant activin A (100 ng/ml for 60 min). Ubiquitinated proteins were captured with FK2 Ab (10 mg; PW8810, Enzo Life Sciences) and protein A/G agarose solution (MilliporeSigma).

RNA sequencing

RNA-seq was performed by MGH Sequencing Core. Libraries were constructed from polyA-selected RNA and sequenced on an Illumina HiSeq2500 instrument. R package DESeq2 was used for gene expression analysis. Genes were considered differentially expressed if changed by $\log_2$FC > +1 or < −1 with an adjusted $P < 0.05$ (after Benjamini-Hochberg correction). Pathway analysis was performed using gene set enrichment analysis (GSEA; Broad Institute) with the Kyoto Encyclopedia of Genes and Genomes database. A false discovery rate of <0.25 was considered significant in GSEA.

Statistical analysis

For the SOMAscan proteomics data, linear regression was performed for each log-transformed, sex-adjusted protein measurement (outcome) versus age. Linear regression models additionally accounted for sample fractions of cases and controls. In the AS cohorts, regression models for NT-proBNP used log-transformed, sex/age-adjusted protein levels, and regression for NYHA was further fit using a linear model with NYHA class used as an ordered factor variable. Protein associations were assessed by partial Pearson's correlations on log-transformed, sex/age-adjusted protein levels. Analyses were performed using SAS software version 9.4. Statistical analyses of human ELISAs and all animal studies were performed using GraphPad Prism 7. Mann-Whitney test, unpaired Student's *t* test, one- or two-way ANOVA with post hoc multiple comparison testing, or Mantel-Cox survival test, were performed as indicated in figure legends. Data are reported as means ± SEM, unless otherwise indicated. $P < 0.05$ was considered statistically significant.

Supplementary Material

Refer to Web version on PubMed Central for supplementary material.

Acknowledgments:

We thank L. Ling (virus construction), Y. Iwamoto (histology), Acceleron (RAP-031), Novartis (CDD866), R. Hajjar (SERCA2a Ab), and NIA (aged mice).

Funding: This work was supported by NIH (AG061034, HL122987, HL135886, TR000901, AR060636, HL132320, and HL080494), AHA (14CSA20500002, 16SFRN31720000, 16FTF29630016, and 14FTF20440012), and Frederick and Ines Yeatts Fund for Innovative Research.

Competing interests: E.L.-T. and D.J.G. are employees and stockholders of Novartis. J.D.R., DJ.G., and A.R. are inventors on a pending patent (PCT/US2018/023390; Methods for Preventing and Treating Heart Disease; WIPO) submitted by BIDMC and Novartis that covers methods for preventing and treating heart disease with activin receptor inhibition. B.R.L. consults for Medtronic and Roche Diagnostics and receives support from Edwards Lifesciences and Roche Diagnostics.

REFERENCES AND NOTES

1. Bui AL, Horwich TB, Fonarow GC, Epidemiology and risk profile of heart failure. Nat. Rev. Cardiol 8, 30–41 (2011). [PubMed: 21060326]
2. Lüscher TF, Heart failure subgroups: HFrEF, HFmrEF, and HFpEF with or without mitral regurgitation. Eur. Heart J 39, 1–4 (2018). [PubMed: 29300945]
3. Shah KS, Xu H, Matsouaka RA, Bhatt DL, Heidenreich PA, Hernandez AF, Devore AD, Yancy CW, Fonarow GC, Heart failure with preserved, borderline, and reduced ejection fraction: 5-year outcomes. J. Am. Coll. Cardiol 70, 2476–2486 (2017). [PubMed: 29141781]
4. Loffredo FS, Steinhauser ML, Jay SM, Gannon J, Pancoast JR, Yalamanchi P, Sinha M, Dall'Osso C, Khong D, Shadrach JL, Miller CM, Singer BS, Stewart A, Psychogios N, Gerszten RE, Hartigan AJ, Kim M-J, Serwold T, Wagers AJ, Lee RT, Growth differentiation factor 11 is a circulating factor that reverses age-related cardiac hypertrophy. Cell 153, 828–839 (2013). [PubMed: 23663781]
5. Olson KA, Beatty AL, Heidecker B, Regan MC, Brody EN, Foreman T, Kato S, Mehler RE, Singer BS, Hveem K, Dalen H, Sterling DG, Lawn RM, Schiller NB, Williams SA, Whooley MA, Ganz P, Association of growth differentiation factor 11/8, putative anti-ageing factor, with cardiovascular outcomes and overall mortality in humans: Analysis of the heart and soul and HUNT3 cohorts. Eur. Heart J 36, 3426–3434 (2015). [PubMed: 26294790]
6. Ganz P, Heidecker B, Hveem K, Jonasson C, Kato S, Segal MR, Sterling DG, Williams SA, Development and validation of a protein-based risk score for cardiovascular outcomes among patients with stable coronary heart disease. JAMA 315, 2532–2541 (2016). [PubMed: 27327800]
7. Sinha M, Jang YC, Oh J, Khong D, Wu EY, Manohar R, Miller C, Regalado SG, Loffredo FS, Pancoast JR, Hirshman MF, Lebowitz J, Shadrach JL, Cerletti M, Kim M-J, Serwold T, Goodyear LJ, Rosner B, Lee RT, Wagers AJ, Restoring systemic GDF11 levels reverses age-related dysfunction in mouse skeletal muscle. Science 344, 649–652 (2014). [PubMed: 24797481]
8. Oshima Y, Ouchi N, Shimano M, Pimentel DR, Papanicolaou KN, Panse KD, Tsuchida K, Lara-Pezzi E, Lee S-J, Walsh K, Activin A and follistatin-like 3 determine the susceptibility of heart to ischemic injury. Circulation 120, 1606–1615 (2009). [PubMed: 19805648]
9. Schafer MJ, Atkinson EJ, Vanderboom PM, Kotajarvi B, White TA, Moore MM, Bruce CJ, Greason KL, Suri RM, Khosla S, Miller JD, Bergen III HR, LeBrasseur NK, Quantification of GDF11 and myostatin in human aging and cardiovascular disease. Cell Metab. 23, 1207–1215 (2016). [PubMed: 27304512]
10. Morissette MR, Stricker JC, Rosenberg MA, Buranasombati C, Levitan EB, Mittleman MA, Rosenzweig A, Effects of myostatin deletion in aging mice. Aging Cell8, 573–583 (2009). [PubMed: 19663901]

11. Jackson MF, Luong D, Vang DD, Garikipati DK, Stanton JB, Nelson OL, Rodgers BD, The aging myostatin null phenotype: Reduced adiposity, cardiac hypertrophy, enhanced cardiac stress response, and sexual dimorphism. J. Endocrinol 213, 263–275 (2012). [PubMed: 22431133]
12. Egerman MA, Cadena SM, Gilbert JA, Meyer A, Nelson HN, Swalley SE, Mallozzi C, Jacobi C, Jennings LL, Clay I, Laurent G, Ma S, Brachat S, Lach-Trifilieff E, Shavlakadze T, Trendelenburg A-U, Brack AS, Glass DJ, GDF11 increases with age and inhibits skeletal muscle regeneration. Cell Metab. 22, 164–174 (2015). [PubMed: 26001423]
13. Smith SC, Zhang X, Zhang X, Gross P, Starosta T, Mohsin S, Franti M, Gupta P, Hayes D, Myzithras M, Kahn J, Tanner J, Weldon SM, Khalil A, Guo X, Sabri A, Chen X, MacDonnell C, Houser SR, GDF11 does not rescue aging-related pathological hypertrophy. Circ. Res 117, 926–932 (2015). [PubMed: 26383970]
14. Zimmers TA, Jiang Y, Wang M, Liang TW, Rupert JE, Au ED, Marino FE, Couch ME, Koniaris LG, Exogenous GDF11 induces cardiac and skeletal muscle dysfunction and wasting. Basic Res. Cardiol 112, 48 (2017). [PubMed: 28647906]
15. Yndestad A, Ueland T, Øie E, Florholmen G, Halvorsen B, Attramadal H, Simonsen S, Frøland SS, Gullestad L, Christensen G, Damås JK, Aukrust P, Elevated levels of activin A in heart failure: Potential role in myocardial remodeling. Circulation 109, 1379–1385 (2004). [PubMed: 14993131]
16. Chen Y, Rothnie C, Spring D, Verrier E, Venardos KM, Kaye DM, Phillips DJ, Hedger MP, Smith JA, Regulation and actions of activin A and follistatin in myocardial ischaemia-reperfusion injury. Cytokine 69, 255–262 (2014). [PubMed: 25052838]
17. Fukushima N, Matsuura K, Akazawa H, Honda A, Nagai T, Takahashi T, Seki A, Murasaki KM, Shimizu T, Okano T, Hagiwara N, Komuro I, A crucial role of activin A-mediated growth hormone suppression in mouse and human heart failure. PLOS ONE 6, e27901 (2011).
18. Greulich S, Maxhera B, Vandenplas G, de Wiza DH, Smiris K, Mueller H, Heinrichs J, Blumensatt M, Cuvelier C, Akhyari P, Ruige JB, Ouwens DM, Eckel J, Secretory products from epicardial adipose tissue of patients with type 2 diabetes mellitus induce cardiomyocyte dysfunction. Circulation 126, 2324–2334 (2012). [PubMed: 23065384]
19. Harrison CA, Al-Musawi SL, Walton KL, Prodomains regulate the synthesis, extracellular localisation and activity of TGF-ß superfamily ligands. Growth Factors 29, 174–186 (2011). [PubMed: 21864080]
20. Walton KL, Makanji Y, Harrison CA, New insights into the mechanisms of activin action and inhibition. Mol. Cell. Endocrinol 359, 2–12 (2012). [PubMed: 21763751]
21. Stamler R, Keutmann HT, Sidis Y, Kattamuri C, Schneyer A, Thompson TB, The structure of FSTL3-activin A complex. Differential binding of N-terminal domains influences follistatin-type antagonist specificity. J. Biol. Chem 283, 32831–32838 (2008). [PubMed: 18768470]
22. Cash JN, Angerman EB, Kattamuri C, Nolan K, Zhao H, Sidis Y, Keutmann HT, Thompson TB, Structure of myostatin·follistatin-like 3: N-terminal domains of follistatin-type molecules exhibit alternate modes of binding. J. Biol. Chem 287, 1043–1053 (2012). [PubMed: 22052913]
23. Tsuchida K, Nakatani N, Hitachi K, Uezumi A, Sunada Y, Ageta H, Inokuchi K, Activin signaling as an emerging target for therapeutic interventions. Cell Commun. Signal 7, 15 (2009). [PubMed: 19538713]
24. Sidis Y, Schneyer AL, Keutmann HT, Heparin and activin-binding determinants in follistatin and FSTL3. Endocrinology 146, 130–136 (2005). [PubMed: 15471966]
25. Bartholin L, Maguer-Satta V, Hayette S, Martel S, Gadoux M, Corbo L, Magaud J-P, Rimokh R, Transcription activation of FLRG and follistatin by activin A, through Smad proteins, participates in a negative feedback loop to modulate activin A function. Oncogene 21, 2227–2235 (2002). [PubMed: 11948405]
26. Bartholin L, Maguer-Satta V, Hayette S, Martel S, Gadoux M, Bertrand S, Corbo L, Lamadon C, Morera A-M, Magaud J-P, Rimokh R, FLRG, an activin-binding protein, is a new target of TGFβ transcription activation through Smad proteins. Oncogene 20, 5409–5419 (2001). [PubMed: 11571638]
27. Ngo D, Sinha S, Shen D, Kuhn EW, Keyes MJ, Shi X, Benson MD, O'Sullivan JF, Keshishian H, Farrell LA, Fifer MA, Vasan RS, Sabatine MS, Larson MG, Carr SA, Wang TJ, Gerszten RE,

Aptamer-based proteomic profiling reveals novel candidate biomarkers and pathways in cardiovascular disease. Circulation 134, 270–285 (2016). [PubMed: 27444932]

28. Afilalo J, Lauck S, Kim DH, Lefévre T, Piazza N, Lachapelle K, Martucci G, Lamy A, Labinaz M, Peterson MD, Arora RC, Noiseux N, Rassi A, Palacios IF, Généreux P, Lindman BR, Asgar AW, Kim CA, Trnkus A, Morais JA, Langlois Y, Rudski LG, Morin J-F, Popma JJ, Webb JG, Perrault LP, Frailty in older adults undergoing aortic valve replacement: The FRAILTY-AVR study. J. Am. Coll. Cardiol 70, 689–700 (2017). [PubMed: 28693934]
29. Dai D-F, Santana LF, Vermulst M, Tomazela DM, Emond MJ, MacCoss MJ, Gollahon K, Martin GM, Loeb LA, Ladiges WC, Rabinovitch PS, Overexpression of catalase targeted to mitochondria attenuates murine cardiac aging. Circulation 119, 2789–2797 (2009). [PubMed: 19451351]
30. Eisenberg T, Abdellatif M, Schroeder S, Primessnig U, Stekovic S, Pendl T, Harger A, Schipke J, Zimmermann A, Schmidt A, Tong M, Ruckenstuhl C, Dammbrueck C,Gross AS, Herbst V, Magnes C, Trausinger G, Narath S, Meinitzer A, Hu Z, Kirsch A, Eller K, Carmona-Gutierrez D, Büttner S, Pietrocola F, Knittelfelder O, Schrepfer E, Rockenfeller P, Simonini C, Rahn A, Horsch M, Moreth K, Beckers J, Fuchs H, Gailus-Durner V, Neff F, Janik D, Rathkolb B, Rozman J, de Angelis MH, Moustafa T, Haemmerle G, Mayr M, Willeit P, von Frieling-Salewsky M, Pieske B, Scorrano L, Pieber T, Pechlaner R, Willeit J, Sigrist SJ, Linke WA, Mühlfeld C, Sadoshima J, Dengiel J, Kiechl S, Kroemer G, Sedej S, Madeo F, Cardioprotection and lifespan extension by the natural polyamine spermidine. Nat.Med 22, 1428–1438 (2016). [PubMed: 27841876]
31. Shahul S, Ramadan H, Nizamuddin J, Mueller A, Patel V, Dreixler J, Tung A, Lang RM, Weinert L, Nasim R, Chinthala S, Rana S, Activin A and late postpartum cardiac dysfunction among women with hypertensive disorders of pregnancy. Hypertension 72, 188–193 (2018). [PubMed: 29844146]
32. Du G-Q, Shao Z-B, Wu J, Yin W-J, Li S-H, Wu J, Weisel RD, Tian J-W, Li R-K, Targeted myocardial delivery of GDF11 gene rejuvenates the aged mouse heart and enhances myocardial regeneration after ischemia-reperfusion injury. Basic Res. Cardiol 112, 7 (2017). [PubMed: 28004242]
33. Rooks D, Praestgaard J, Hariry S, Laurent D, Petricoul O, Perry RG, Lach-Trifilieff E, Roubenoff R, Treatment of sarcopenia with Bimagrumab: Results from a phase II, randomized, controlled, proof-of-concept study. J. Am. Geriatr. Soc 65, 1988–1995 (2017). [PubMed: 28653345]
34. Morvan F, Rondeau J-M, Zou C, Minetti G, Scheufler C, Scharenberg M, Jacobi C, Brebbia B, Ritter V, Toussaint G, Koelbing C, Leber X, Schilb A, Witte F, Lehmann S, Koch E, Geisse S, Glass DJ, Lach-Trifileff E, Blockade of activin type II receptors with a dual anti-ActRIIA/IIB antibody is critical to promote maximal skeletal muscle hypertrophy. Proc. Natl. Acad. Sci. U.S.A 114, 12448–12453 (2017). [PubMed: 29109273]
35. Schmitt JP, Debold EP, Ahmad F, Armstrong A, Frederico A, Conner DA, Mende U, Lohse MH, Warshaw D, Seidman CE, Seidman JG, Cardiac myosin missense mutations cause dilated cardiomyopathy in mouse models and depress molecular motor function. Proc. Natl. Acad. Sci. U.S.A 103, 14525–14530 (2006). [PubMed: 16983074]
36. Campbell C, McMillan HJ, Mah JK, Tarnopolsky M, Selby K, McClure T, Wilson DM, Sherman ML, Escolar D, Attie KM, Myostatin inhibitor ACE-031 treatment of ambulatory boys with Duchenne muscular dystrophy: Results of a randomized, placebo-controlled clinical trial. Muscle Nerve 55, 458–464 (2017). [PubMed: 27462804]
37. Lee S-J, McPherron AC, Regulation of myostatin activity and muscle growth. Proc. Natl. Acad. Sci. U.S.A 98, 9306–9311 (2001). [PubMed: 11459935]
38. Zhu H, Kavsak P, Abdollah S, Wrana JL, Thomsen GH, A SMAD ubiquitin ligase targets the BMP pathway and affects embryonic pattern formation. Nature 400, 687–693 (1999). [PubMed: 10458166]
39. Dogra D, Ahuja S, Kim H-T, Rasouli SJ, Stainier DYR, Reischauer S, Opposite effects of activin type 2 receptor ligands on cardiomyocyte proliferation during development and repair. Nat. Commun 8, 1902 (2017). [PubMed: 29196619]
40. Zhou X, Wang JL, Lu J, Song Y, Kwak KS, Jiao Q, Rosenfeld R, Chen Q, Boone T, Simonet WS, Lacey DL, Goldberg AL, Han HQ, Reversal of cancer cachexia and muscle wasting by ActRIIB antagonism leads to prolonged survival. Cell 142, 531–543 (2010). [PubMed: 20723755]

41. Rothman AMK, Arnold ND, Pickworth JA, Iremonger J, Ciuclan L, Allen RMH, Guth-Gundel S, Southwood M, Morrell NW, Thomas M, Francis SE, Rowlands DJ, Lawrie A, MicroRNA-140–5p and SMURF1 regulate pulmonary arterial hypertension. J. Clin. Invest 126, 2495–2508 (2016). [PubMed: 27214554]

42. Miyamoto MI, del Monte F, Schmidt U, DiSalvo TS, Kang ZB, Matsui T, Guerrero JL, Gwathmey JK, Rosenzweig A, Hajjar RJ, Adenoviral gene transfer of SERCA2a improves left-ventricular function in aortic-banded rats in transition to heart failure. Proc. Natl. Acad. Sci. U.S.A 97, 793–798 (2000). [PubMed: 10639159]

43. Kho C, Lee A, Jeong D, Oh JG, Chaanine AH, Kizana E, Park WJ, Hajjar RJ, SUMO1-dependent modulation of SERCA2a in heart failure. Nature 477, 601–605 (2011). [PubMed: 21900893]

44. Hartupee J, Mann DL, Neurohormonal activation in heart failure with reduced ejection fraction. Nat. Rev. Cardiol 14, 30–38 (2017). [PubMed: 27708278]

45. Boström P, Mann N, Wu J, Quintero PA, Plovie ER, Panáková D, Gupta RK, Xiao C, MacRae CA, Rosenzweig A, Spiegelman BM, C/EBPβ controls exercise-induced cardiac growth and protects against pathological cardiac remodeling. Cell 143, 1072–1083 (2010). [PubMed: 21183071]

46. Tan SM, Zhang Y, Connelly KA, Gilbert RE, Kelly DJ, Targeted inhibition of activin receptor-like kinase 5 signaling attenuates cardiac dysfunction following myocardial infarction. Am. J. Physiol. Heart Circ. Physiol 298, H1415–H1425 (2010). [PubMed: 20154262]

47. Lee S-J, Huynh TV, Lee Y-S, Sebald SM, Wilcox-Adelman SA, Iwamori N, Lepper C, Matzuk MM, Fan C-M, Role of satellite cells versus myofibers in muscle hypertrophy induced by inhibition of the myostatin/activin signaling pathway. Proc. Natl. Acad. Sci. U.S.A 109, E2353–E2360 (2012). [PubMed: 22869749]

48. Kijlstra JD, Hu D, Mittal N, Kausel E, van der Meer P, Garakani A, Domian IJ, Integrated analysis of contractile kinetics, force generation, and electrical activity in single human stem cell-derived cardiomyocytes. Stem Cell Rep. 5, 1226–1238 (2015).

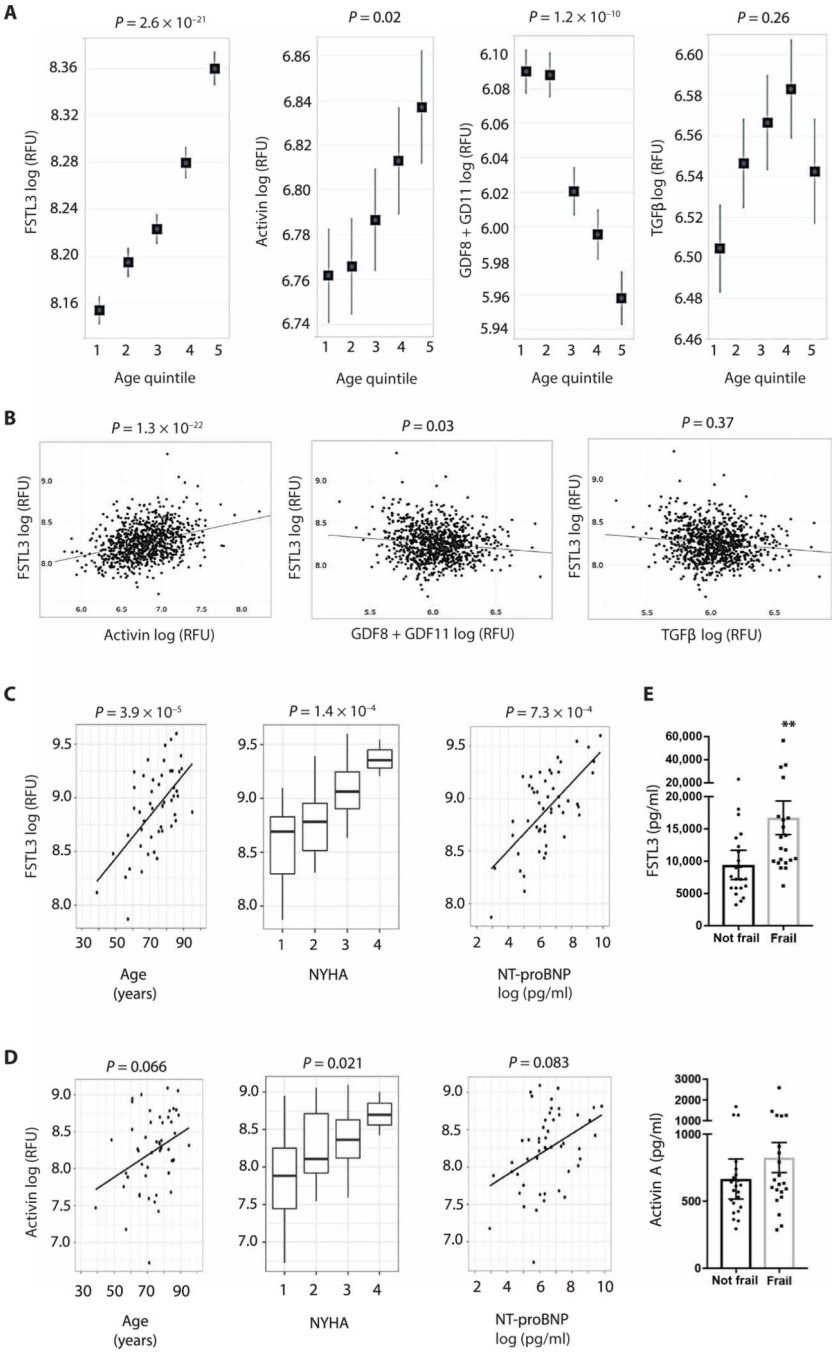

Fig. 1. Circulating FSTL3 and activins increase in human aging and HF.

(**A**) Linear regression of plasma FSTL3, activin, GDF8 + GDF11, and TGFβ with increasing quintiles (Q) of age in the FHS cohort [Q1, 29 to 47 years (n = 172); Q2, 47 to 52 years (n = 183); Q3, 53 to 59 years (n = 181); Q4, 60 to 65 years (n = 184); Q5, 66 to 82 years (n = 179)]. Data are shown as means ± SEM. (**B**) Partial Pearson's correlations of FSTL3 with activin, GDF8 + GDF11, and TGFβ in the FHS cohort. (**C**) Linear regression of plasma FSTL3 with age, NYHA class, or NT-proBNP in the AS/HF cohort (n = 50). (**D**) Linear regression of plasma activins with age, NYHA class, or NT-proBNP in the AS/HF cohort.

(**E**) Plasma FSTL3 and activin A concentrations [measured by enzyme-linked immunosorbent assay (ELISA)] in an independent cohort of older patients with AS phenotyped for frailty ($n = 43$). Data are shown as means ± SEM. $^{**}P < 0.01$ by Mann-Whitney test. In (A) to (D), proteins measured with SomaLogic aptamers and displayed as log-transformed relative fluorescence units (RFU). Protein measurements are sex-adjusted when plotted against age, otherwise age and sex adjusted.

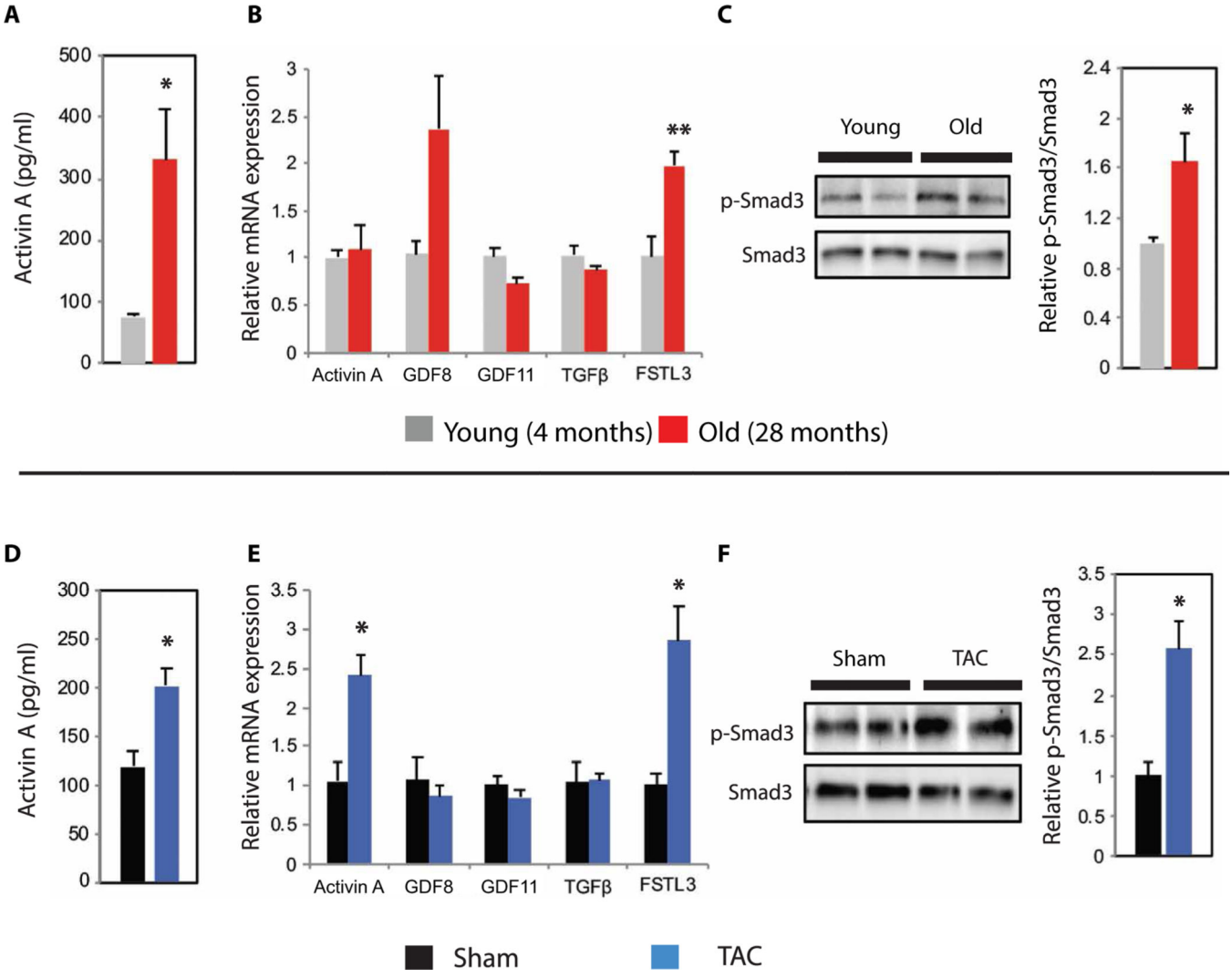

Fig. 2. Circulating activin A and cardiac ActRII signaling increase in murine aging and LV pressure overload.

(**A** to **C**) Comparison of young (4 months; gray) versus old (28 months; red) C57BL/6 males. (A) Plasma activin A concentrations in young ($n = 6$) versus old ($n = 9$). (B) Relative cardiac mRNA expression of ActRII ligands, TGFβ, and FSTL3 in young ($n = 4$) versus old ($n = 8$). (C) Representative immunoblot and relative quantification of cardiac p-Smad3 and total Smad3 expression in young ($n = 4$) versus old ($n = 4$). (**D** to **F**) Comparison of 4-month-old C57BL/6 males 1 week after Sham versus TAC surgery. $n = 3$ per group for all analyses. (D) Plasma activin A concentrations. (E) Relative cardiac mRNA expression of ActRII ligands, TGFb, and FSTL3. (F) Representative immunoblot and relative quantification of cardiac p-Smad3 and total Smad3 expression. For all panels, data are shown as means ± SEM. $^{*}P < 0.05$, $^{**}P < 0.01$ by Student's t test.

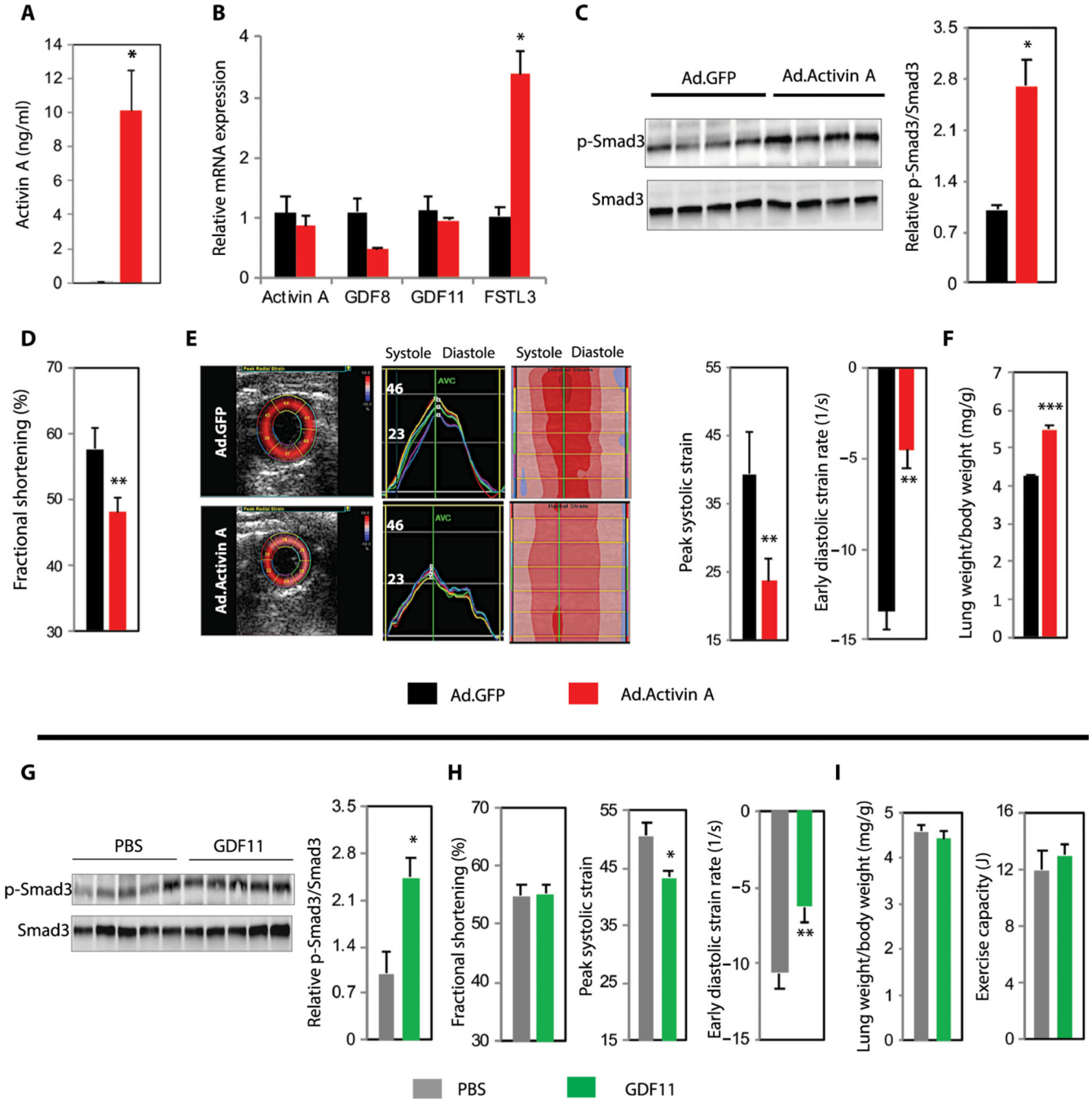

Fig. 3. Increased circulating ActRII ligands are sufficient to induce cardiac dysfunction.

(**A** to **F**) Young (4 months) C57BL/6 males injected with either Ad.GFP (black) or Ad.activin A (red). $n = 4$ per group for all analyses. (A) Plasma activin A concentration 96 hours after infection. (B) Relative cardiac mRNA expression of ActRII ligands and FSTL3. (C) Immunoblot and relative quantification of cardiac p-Smad3/Smad3. (D) Fractional shortening (FS) by echocardiography. (E) Representative echocardiographic strain images and quantification of radial systolic strain and early diastolic strain rates. (F) Lung weight normalized to body weight. (**G** to **I**) Old (24 months) C57BL/6 males treated with daily

intraperitoneal injections of phosphate-buffered saline (PBS) (n = 8; gray) versus GDF11 (0.1 mg/kg) (n = 8; green) for 28 days. Two mice died before study completion. (G) Immunoblot and relative quantification of cardiac p-Smad3/Smad3. n = 5 per group. (H) Echocardiographic FS, radial strain, and strain rate analyses. n = 6 to 7 per group. (I) Lung weight/body weight and exercise capacity. n = 7 per group. For all panels, data are shown as means ± SEM. $*P < 0.05$, $**P < 0.01$, $***P < 0.001$ by Student's t test.

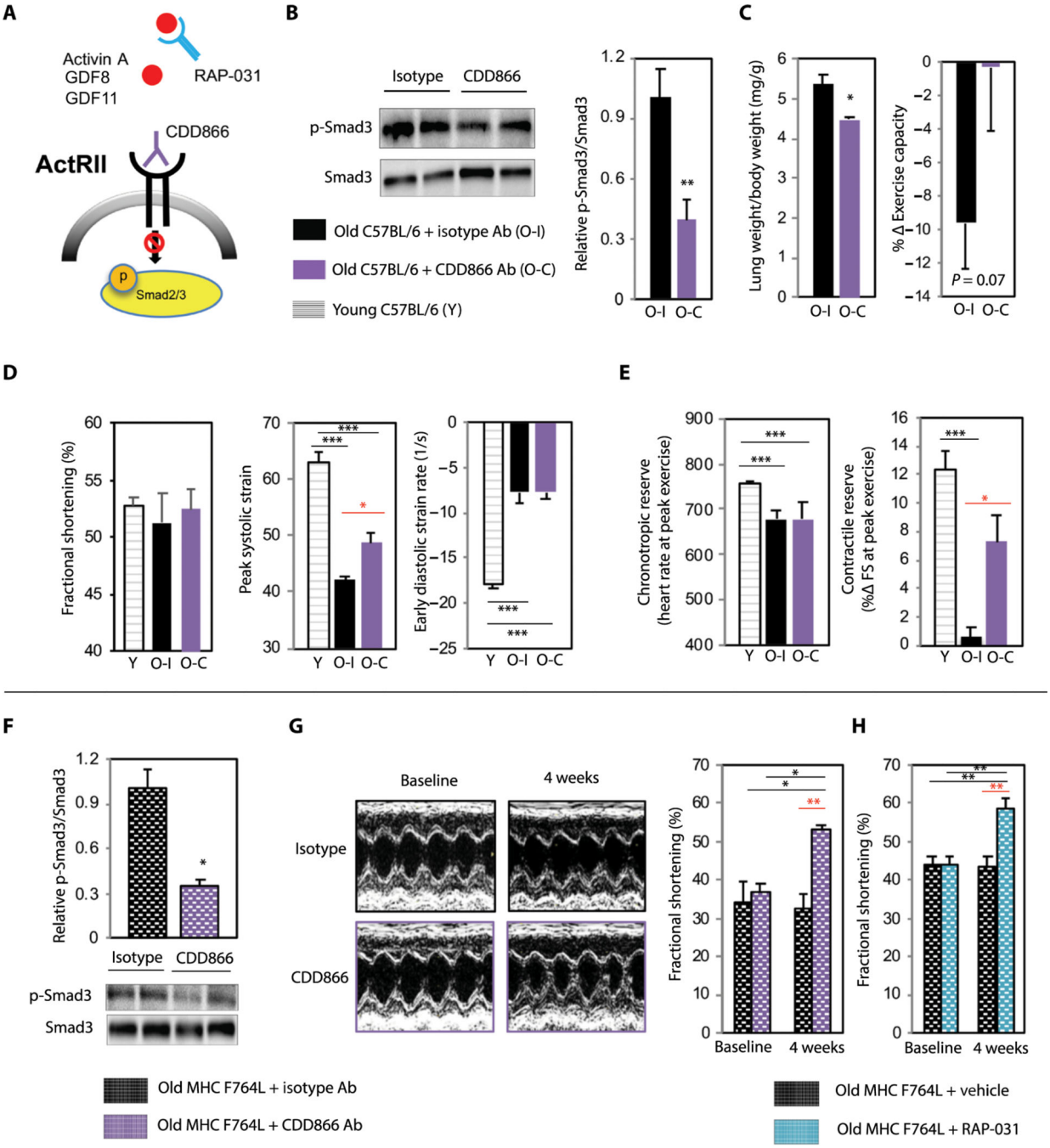

Fig. 4. ActRII pathway inhibition improves systolic function in age-related HF in mice.

(**A**) Schematic depicting ActRII pathway inhibitors used. (**B** to **E**) Old (24 months) C57BL/6 males treated with weekly injection of isotype (O-I; $n = 6$; black) versus CDD866 (O-C; $n = 7$; purple) for 4 weeks. Young (4 months) C57BL/6 males (Y; $n = 12$; striped) used for comparison in cardiac functional testing. (B) Representative immunoblot and relative quantification of cardiac p-Smad3/Smad3. $n = 6$ per group. (C) HF phenotyping. Lung weight normalized to body weight. Percentage change in exercise capacity (compared to pretreatment). $n = 6$ to 7 per group. (D) Resting cardiac function (% FS strain analyses)

by echocardiography. $n = 5$ to 12 per group. (E) Cardiac reserves at peak exercise. $n = 5$ to 12 per group. (**F** and **G**) Old (21 to 23 months) MHCF764L mice (mixed genders) treated with isotype ($n = 3$; black) versus CDD866 ($n = 5$; purple) for 4 weeks. (F) Representative immunoblot and relative quantification of cardiac p-Smad3/Smad3. $n = 3$ per group. (G) Representative echocardiographic images and the FS at baseline and 4 weeks. $n = 3$ to 5 per group. (**H**) Old (18 to 20 months) MHCF764L mice (mixed genders) treated with vehicle ($n = 6$; black) versus RAP-031 ($n = 6$; blue). FS at baseline and 4 weeks. Data in all panels are shown as means ± SEM. $*P < 0.05$, $**P < 0.01$, $***P < 0.001$ by Student's t test (B, C, and F), one-way analysis of variance (ANOVA) with post hoc Tukey (D and E), and two-way ANOVA with post hoc Sidak (G and H).

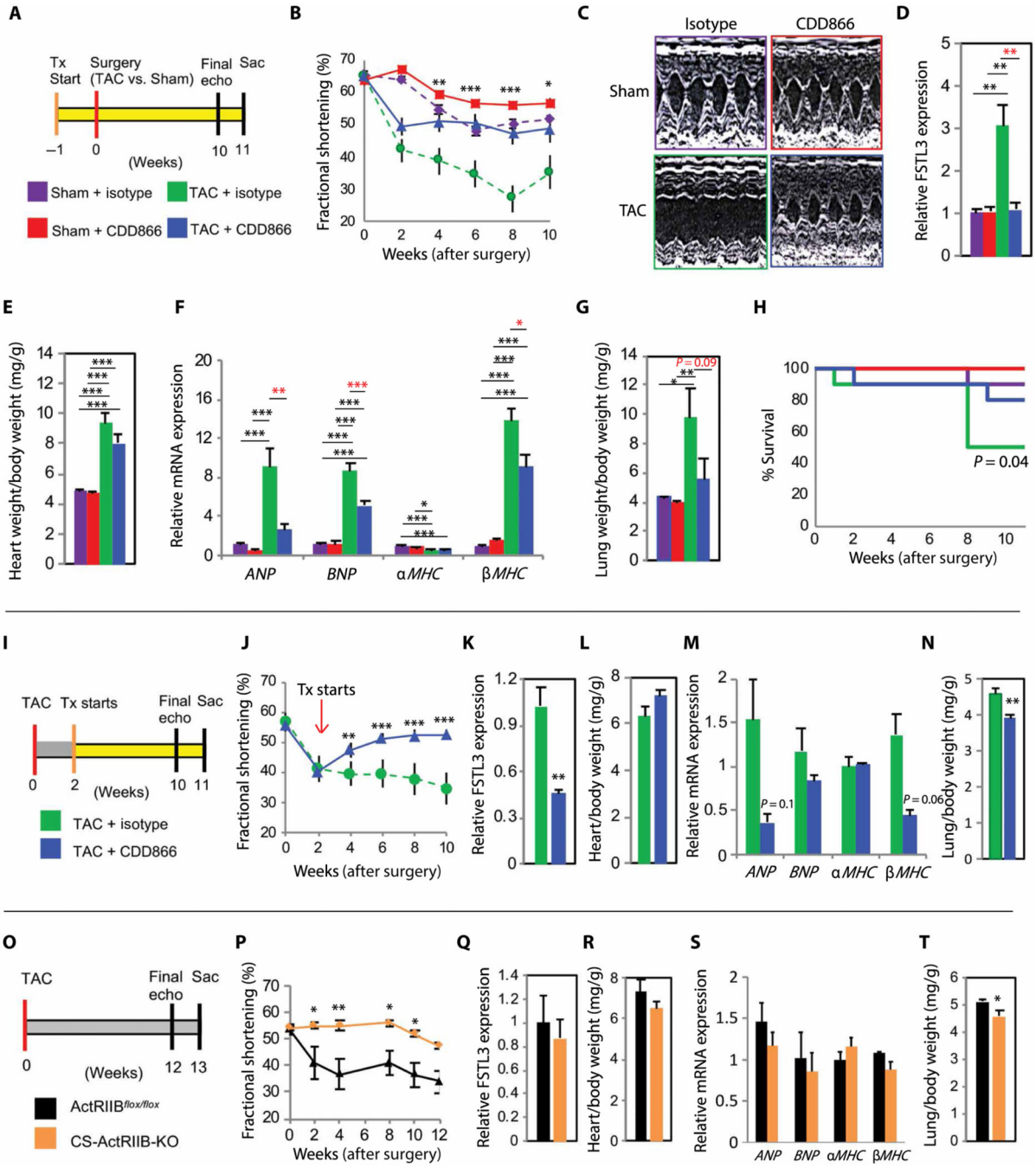

Fig. 5. ActRII inhibition improves systolic function in TAC.

(**A** to **H**) Prevention study. Weekly treatment (isotype versus CDD866) started 1 week before surgery (Sham versus TAC). *n* = 10 per group. (A) Prevention protocol. Sac, sacrifice. (B) Serial FS over 10 weeks. Analysis displayed for TAC-isotype versus TAC-CDD866. *n* = 5 to 10 per group per time point. (C) Representative echocardiographic images at 10 weeks. (D) Relative cardiac FSTL3 mRNA expression. *n* = 6 to 9 per group. (E) Heart weight normalized to body weight. *n* = 8 to 10 per group. (F) Gene expression profile of pathologic hypertrophy. *n* = 6 to 9 per group. (G) Lung weight normalized to body weight. *n* = 8 to 10

per group. (H) Mantel-Cox survival curve (mortality, natural death or euthanasia due to FS ≤ 20%). (**I** to **N**) Treatment study. Weekly treatment (isotype, $n = 5$, versus CDD866, $n = 7$) started after FS < 45%. $n = 5$ to 7 per group for all analyses. (I) Treatment protocol. (J) Serial FS over 10 weeks. (K) Relative cardiac FSTL3 mRNA expression. (L) Heart/body weight. (M) Gene expression profile of pathologic hypertrophy. (N) Lung/body weight. (**O** to **T**) CS-ActRIIB-KO TAC study. ActRIIB$^{flox/flox}$ ($n = 6$) and CS-ActRIIB-KO (n = 5) mice subjected to TAC for 12 weeks. $n = 5$ to 6 per group for analyses. (O) CS-ActRIIB-KO TAC protocol. (P) Serial FS over 12 weeks. (Q) Relative cardiac FSTL3 mRNA expression. (R) Heart/body weight. (S) Gene expression profile of pathologic hypertrophy. (T) Lung/body weight. Data are shown as means ± SEM. *$P < 0.05$, **$P < 0.01$, ***$P < 0.001$ by one-way ANOVA with post hoc Tukey (C to G), two-way ANOVA with post hoc Tukey (B), Student's *t* test (K to N and Q to T), and two-way ANOVA with post hoc Sidak (J and P).

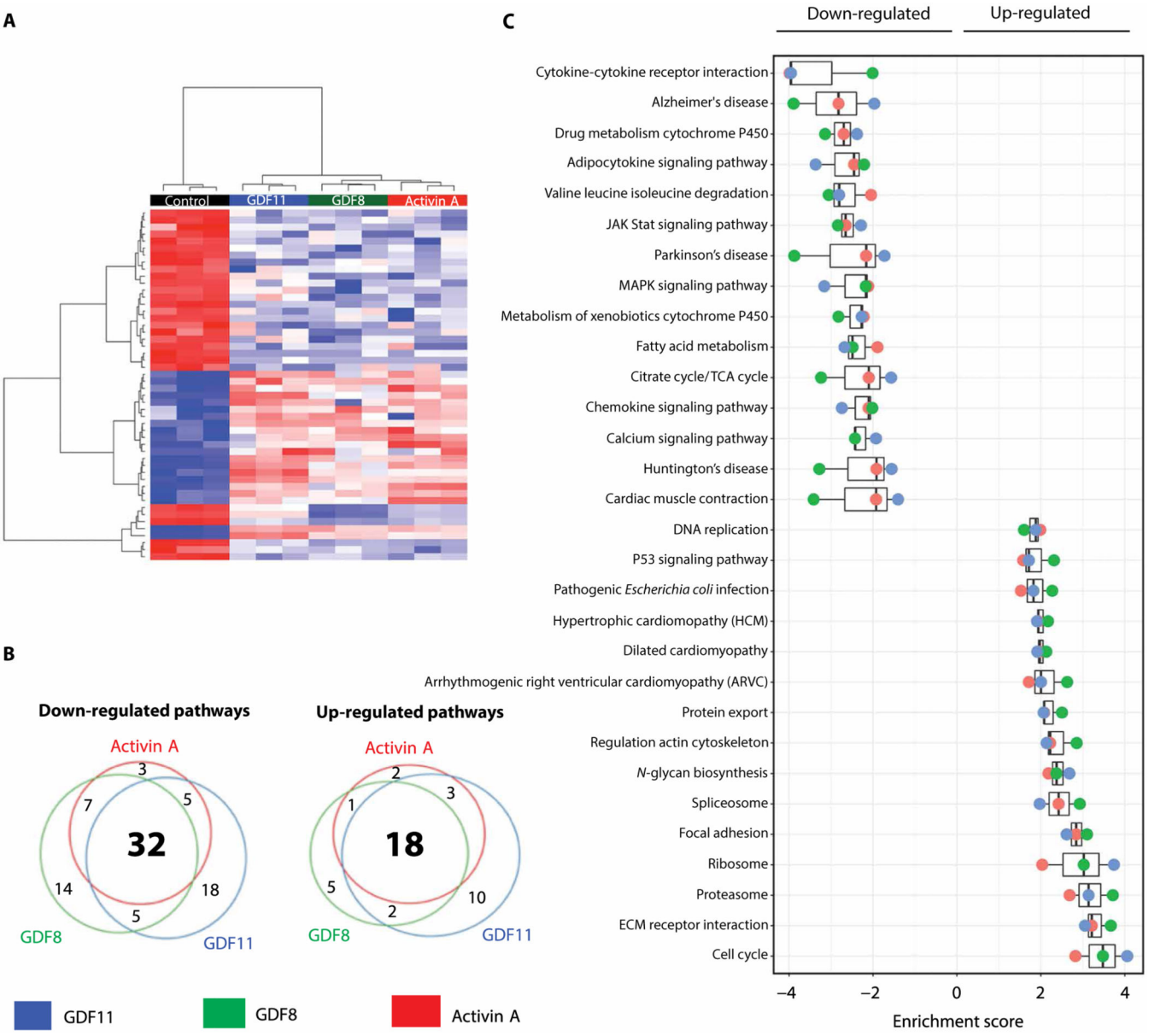

Fig. 6. ActRII ligands induce similar pathologic profile in mammalian CMs.

NRVMs incubated with GDF11, GDF8, or activin A (100 ng/ml) for 18 hours. $n = 3$ per group. (**A**) Heat map of most highly differentially expressed genes [log2(FC) > 2; $P_{adj} <$ 0.05]. (**B**) Venn diagrams of differentially regulated pathways (false discovery rate, <0.25). (**C**) Enrichment scores of most highly differentially regulated pathways by all three ligands. TCA, tricarboxylic acid.

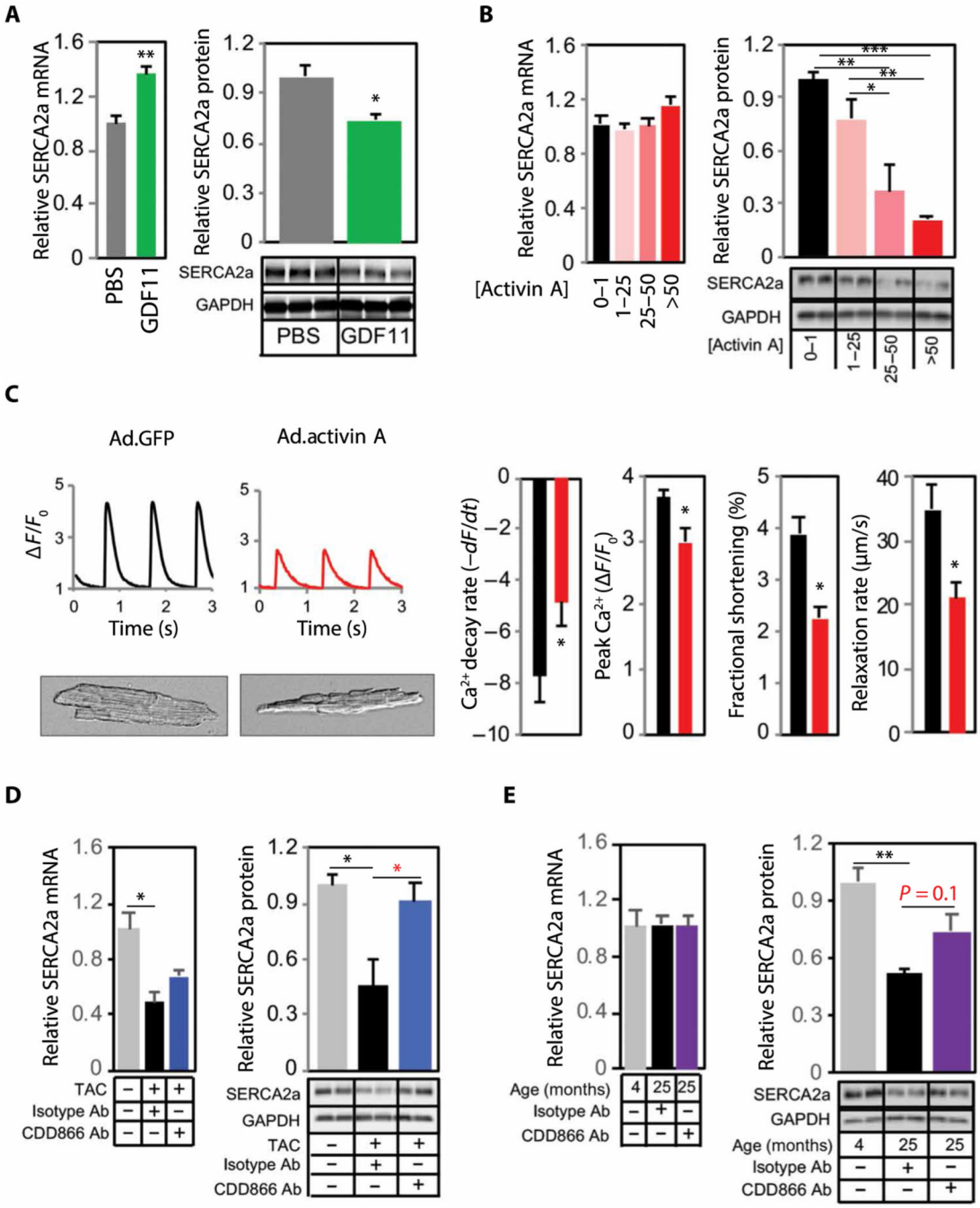

Fig. 7. ActRII signaling modulates SERCA2a expression in the heart.

(**A**) Relative cardiac SERCA2a mRNA and protein expression in old (24 months) C57BL/6 from GDF11 substudy (Fig. 3). $n = 5$ to 6 per group. GAPDH, glyceraldehyde-3-phosphate dehydrogenase. (**B**) Relative cardiac SERCA2a mRNA and protein expression in 4-month-old C57BL/6 infected with Ad.GFP (black) versus Ad.activin A (pink red). Quartiles based on plasma activin A concentrations (nanograms per milliliter) at 96 hours. $n = 4$ per group. (**C**) Adult CMs isolated from mice infected with Ad.GFP ($n = 3$; black) versus Ad.activin A ($n = 5$; red). Representative images and Ca^{2+} flux curves and quantification of Ca^{2+} decay

rate (from 25 to 75% diastole), peak Ca^{2+}, contractility (FS), and relaxation rate (from 25 to 75% diastole). $n = 7$ to 24 CM per mouse. Data are shown as average CM per mouse. (**D**) Relative cardiac SERCA2a mRNA and protein expression in 4-month-old C57BL/6 subjected to TAC and treated with isotype ($n = 7$; black) versus CDD866 ($n = 8$; blue) for 1 week after FS of <45%. No surgery control ($n = 4$; gray). (**E**) Relative cardiac SERCA2a mRNA and protein expression in old (24 months) C57BL/6 treated with isotype ($n = 4$; black) versus CDD866 ($n = 4$; purple) for 4 weeks. Untreated young control (4 months; $n = 4$; gray). Data are shown as means ± SEM. *$P < 0.05$, **$P < 0.01$, ***$P < 0.001$ by Student's *t* test (A and C) and one-way ANOVA with post hoc Tukey (B, D, and E).

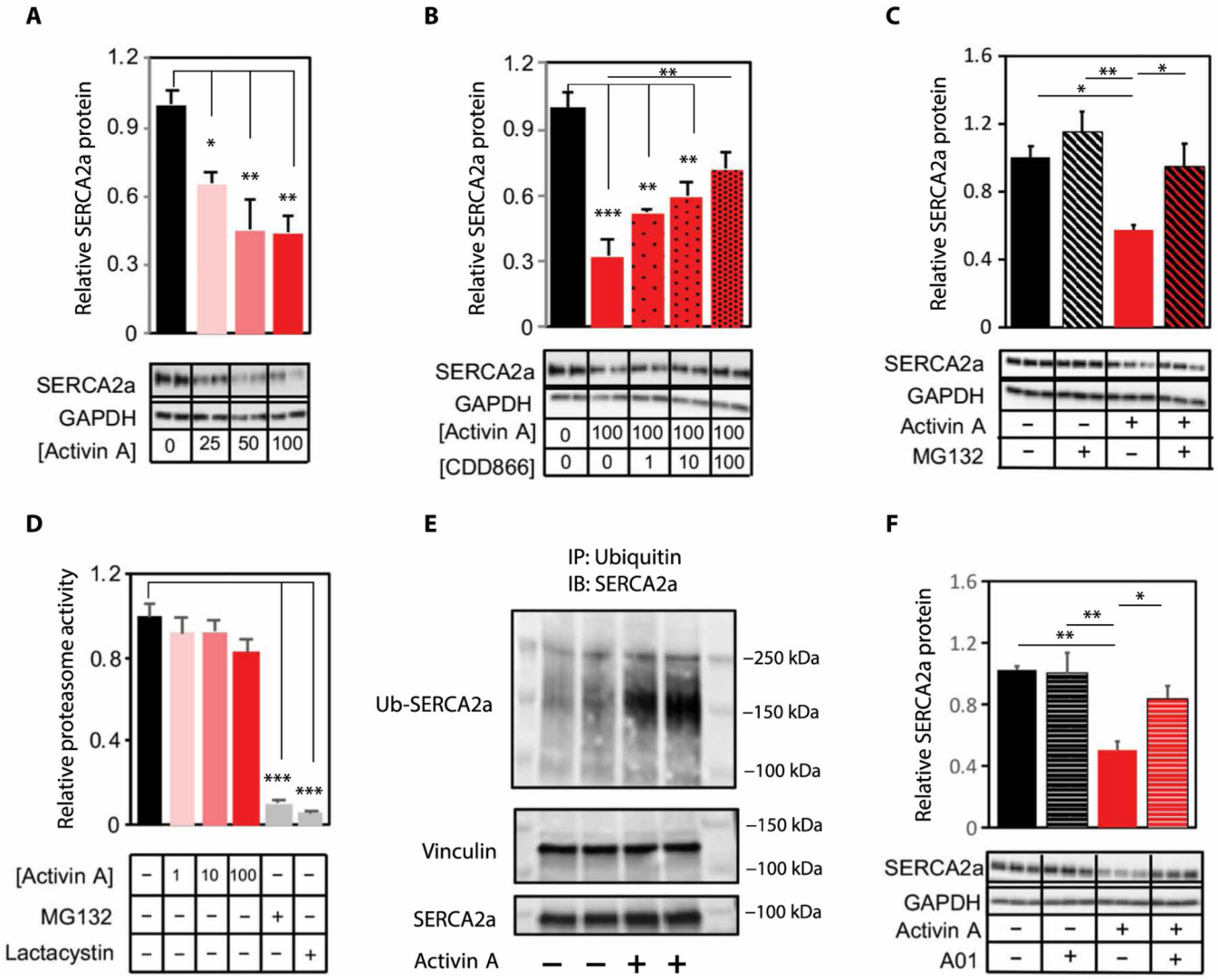

Fig. 8. Activin/ActRII signaling modulates proteasome-mediated SERCA2a degradation via E3 ligase Smurf1.

Representative immunoblot and quantification of relative SERCA2a protein content in NRVMs incubated with (**A**) activin A (0 to 100 ng/ml), $n = 2$ to 3 per group (repeated three times)]; (**B**) activin A (0 ng/ml versus 100 ng/ml) and CDD866 (0 to 100 μg/ml), $n = 3$ per group; or (**C**) activin A (0 ng/ml versus 100 ng/ml) and MG132 (0 μM versus 10 μM), $n = 3$ per group (repeated three times). (**D**) Proteasome activity in NRVM incubated with activin A (0 to 100 ng/ml). $n = 2$ to 3 per group (repeated two times). Proteasome inhibitors, MG132, and lactacystin were used as internal controls. (**E**) Top: Representative immunoblot (IB) of ubiquitinated (Ub) SERCA2a. Bottom: SERCA2a and vinculin immunoblots from same lysates without immunoprecipitation (IP) . (**F**) Representative immunoblot and quantification of relative SERCA2a protein in NRVMs incubated with activin A (0 ng/ml versus 100 ng/ml) and Smurf1 inhibitor A01 (0 uM versus 10 uM). $n = 3$ per group (repeated three times). All inhibitor experiments were performed with 6-hour pretreatment with inhibitors (CDD866, MG132, or A01), followed by 18-hour activin A incubation. IP (E) was done with a 1-hour activin A incubation. Data are shown as means ± SEM and were

calculated from average of replicate experiments. *$P < 0.05$, **$P < 0.01$, ***$P < 0.001$ by one-way ANOVA with post hoc Tukey (A, B, C, and F) or Dunnett (D).